Defect Detection and Classification of Electronic Circuit Boards Using Keypoint Extraction and CNN Features

Yohei Takada Tokiko Shiina Hiroyasu Usami Yuji Iwahori

Department of Computer Science
Chubu University
Kasugai, 487-8501 Japan
email:{ytakada|shiina|usami}@cvl.cs.chubu.ac.jp
email:iwahori@cs.chubu.ac.jp

M. K. Bhuyan

Dept. of Electronics
and Electrical Engineering
Indian Institute of Technology Guwahati
Guwahati, 781039 India
email:mkb@iitg.ernet.in

***Abstract*—This paper proposes a method for defect detection and classification of electronic circuit board by extracting keypoints without reference images. The final purpose is to distinguish a problematic defect, such as disconnection from a non-defect, dust in the manufacturing process et al. Keypoints are extracted from the electronic circuit board image, then a patch image is cropped using obtained keypoint information, such as the position. The cropped images are used as input to CNN (Convolutional Neural Network) and 4096-dimensional features are obtained in the final layer of the full connected layers. SVM (Support Vector Machine) is introduced for learning and classification using CNN features. The effectiveness of the proposed method is confirmed through a detection experiment using actual electronic circuit board images containing defects and by comparing the results with the previous method.**

Keywords–Defect Detection; Defect Classification; CNN; SVM; SURF.

I. INTRODUCTION

Electronic circuit boards are used as components of various precision instruments, such as computers and liquid crystal displays. Each layer is inspected after drawing and baking the mask pattern in the manufacturing process of the electronic circuit boards. There is Automated Optical Inspection (AOI) as a computer assisted automated visual inspection for circuit boards. The defect is judged from the loss rate of the lead wire portion in AOI, but the final goal is to determine if that defect is a true or a pseudo defect of the product. The inspections need to be done with high accuracy. The current AOI needs a subsequent final verification by the human eye to judge the existence of a defect. The human cost and variability of the inspection accuracy originating from individual checking ability are problems in the verification process. It is hoped to reduce this cost and to keep the accuracy for inspection with computer-aided defect inspection.

Defect types during the inspection consist of true defect and pseudo defect. True defects include chipping, breaking, protrusions, shorts, etc. True defects cannot be shipped as the products when these defects are found. On the other hand, pseudo defects have foreign matter adherence and stains and these can be removed after inspection. So, pseudo defets can be shipped as the product. If a true defect is erroneously classified into a pseudo defect, it becomes a problem. If a pseudo defect is erroneously classified as a true defect, the product will be discarded. Normal products are disposed of when a pseudo defect is erroneously classified as a true defect, and it causes reduction of production yield rate.

Papers [1] and [2] have been proposed to solve these problems using image processing. Paper [1] proposes a global defect inspection of defects by learning using Mahalanobis distance. Paper [2] supplies a current to the electronic circuit boards, and the defect is detected from the radiation position from the radiation infrared image by taking advantage of the characteristic that the short portion generates heat due to the leak current.

The works [3] - [4] have proposed the defect classification. Paper [3] classifies defect type using its shape informatio-nunder the assumption that the reference image is used for the classification. Paper [5] detects a candidate region of defect by taking the difference between the reference image and the test image. Feature quantities are obtained from the candidate region and two classes classification of true defect and pseudo defect is proposed using SVM. Mutiple subsets are constructed by random sampling of the dataset,thenn multiple classifiers are constructed based on each subsets feature. The data classification is performed by taking a majorityvote, and the stable accuracy is obtained if the number of learningdata is sufficient. However, it is necessary to prepare the reference images under inspection. The creation of the reference image requires positioning in units of pixels, and it costs much to create a reference image for each inspection image. Paper [4] proposes a defect classification method using Bag-of-Features as a method without using a reference image, while this paper deals with AVI (Automatic Visual Inspection) which is available to the simpler patterns of electronic circuit boards. The method cannot be directly applied to AOI.

This paper tries to improve the accuracy of detection and classification using features obtained by Convolutional Neural Network (CNN). The candidate defect region is extracted without reference image by keypoint extraction in defect classification, and features are extracted by inputting the cropped region into the CNN.

II. TYPES OF DEFECT

True defect and pseudo defect are classified into several types depending on the color and shape of the defect portion.

 ISBN: 978-1-61208-534-0

A defect of the same type often has some variation based on the image, and this makes it difficult to classify it as a true or pseudo defect.

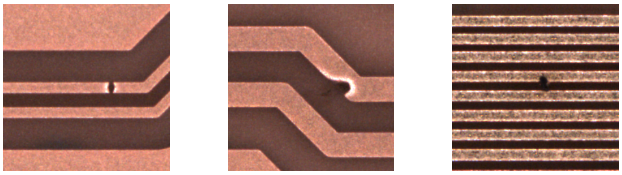

(a) Disconnection (b) Crack (c) Crack

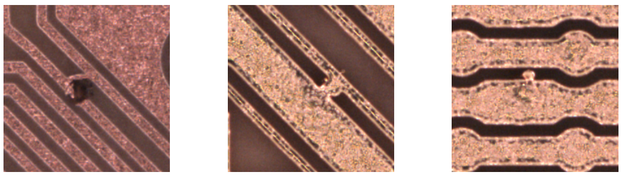

(d) Connection (e) Connection (f) Projection

Figure 1. Type of True Defects

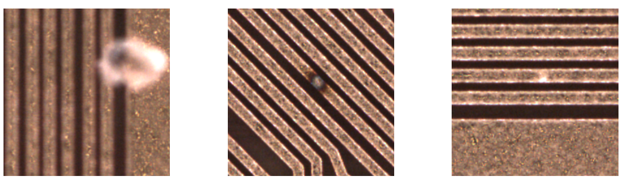

(a) Dust (b) Stain (c) Stain

Figure 2. Type of Pseudo Defects

It is confirmed that there is a difference in the intensity value of the edge portion in the crack defect as shown in Figure 1(b) and Figure 1(c). The connected part is thinner than the normal lead wire as shown in Figure 1(d), while a thicker part than the normal lead is observed in connection defect as shown in Figure 1(e). The appearance also differs even in the pseudo defect. It is confirmed that there is a difference in the radiance value of the defect part in the Figure 2(b) and Figure 2(c) which are stain defect. It is also confirmed that noise appears in the entire image.

III. INSPECTION METHOD USING REFERENCE IMAGE

In [5], a non-defect reference image is prepared for an image to be inspected. A difference is taken for each RGB channel and a binary conversion is performed on the difference image using a threshold value obtained from a discriminant analysis method. The defect region is detected by taking the logical sum of three binarized images (Figure (3)). Since the reference image should be aligned on a pixel-by-pixel basis at the time of creation and there may be multiple similar portions in the same electronic board, it takes cost to obtain the difference from the correct portion. The example result of defect detection using both inspection image and reference image is shown in Figure 3(c).

Feature quantities, such as maximum value, median value, mode value, and so on are extracted as a feature quantity from the detected defect region in each channel of RGB and HSV

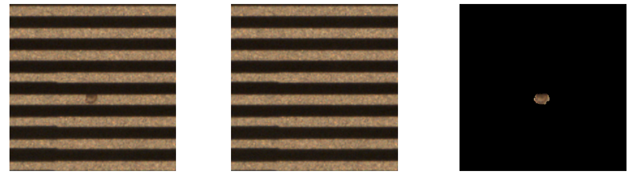

(a) Inspection Image (b) Reference Image (c) Result of Detection

Figure 3. Detection of Defect

(Hue, Saturation, Value) and so on. Subsets are created from the entire dataset using random sampling and multiple SVMs are constructed. The final result is decided by the majority vote using multiple SVMs.

IV. PROPOSED METHOD

The proposed method uses SURF, which is a keypoint extraction method, and extracts a defect candidate region without reference images. Features are obtained by inputting the extracted region to CNN, which is a feature extraction processing of Deep Learning. Both SVMs for defect detection and defect classification are constructed using the obtained features, and these SVMs perform defect detection and defect classification, respectively.

The procedure of the proposed method is as follows.

1) Convert the learning image to the HSV color representation system and detect the feature for the S channel using SURF.
2) Create a rectangle using the coordinates and scale of the obtained keypoint, and crop the image.
3) Label the image cropped from the defect portion or non-defect portion using the reference image.
4) Obtain features from the final layer of the full connected layer of CNN by inputting the cropped image to CNN.
5) Construct SVM for defect detection by using the features obtained from the defect portion and the features obtained from the non-defect portion.
6) Construct SVM for defect classification by separating the features obtained from defect region into true defect and pseudo defect.

A. Determination of Pseudo Defect Region Using Keypoint Extraction

SURF is a method to extract features which are invariant to the illumination change, the scale change or the rotation. Keypoints are detected by creating multiple DoG (Difference of Gaussian) images and detecting the local maximum value of intensity in SURF. The value of scale σ is also used to obtain the orientation of the keypoint. SURF is a rotationally invariant feature by normalizing direction in orientation. The gradient direction is determined within the circle region whose radius is obtained by multiplying the scale σ of the keypoint by six times.

SURF obtains the S channel after converting the input image to HSV color system. As a result, the S channel was adopted from the experience that the keypoint detected from the defect region gained the common point where the gradient strength becomes strong when obtaining SURF.

 ISBN: 978-1-61208-534-0

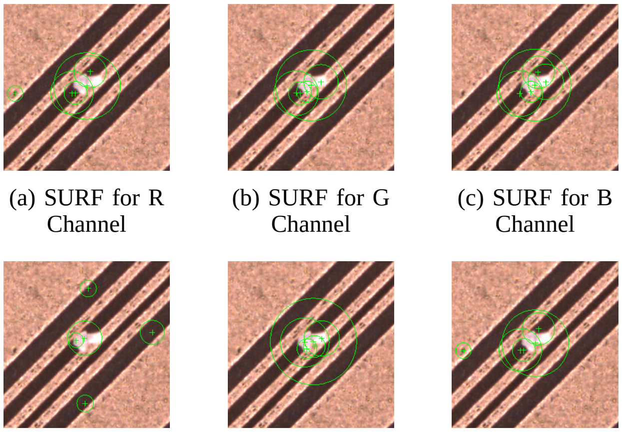

(a) SURF for R Channel (b) SURF for G Channel (c) SURF for B Channel

(d) SURF for H Channel (e) SURF for S Channel (f) SURF for V Channel

Figure 4. SURF Features

At first sight, observation shows that the keypoint is concentrated on the defect in the three channels of RGB (Figure 4(a), 4(b) and 4(c), but the keypoint was detected at the position deviating from the defect when the result is exactly confirmed with the mask image. It is confirmed that the keypoint concentrates on the defect at the result of the S channel (Figure 4(e)), and all five keypoints were detected on the defect region when the result is exactly confirmed with mask image. This characteristic was confirmed with more than 90% of dataset images.

B. Cropping Defect Candidate Image

Defect candidate images are cropped by SURF, as explained in Section IV-A. An image is cropped using a rectangle that encloses a circle with a radius of $6 \times \sigma$ used when orientation is determined by SURF. The number of keypoints used for a rectangle cropping in a test image is determined by the following procedure.

1) The keypoints detected from the learning image I_n is sorted in descending order of the gradient strength.
2) The keypoints are plotted in order of sorting for the mask image created from the learning image I_n and the reference image.
3) Record the number of the keypoint which is first plotted in the defect region of the mask image.
4) 1) to 3) are applied to all learning images, and the average value of the keypoint numbers recorded is used for cropping the rectangle in a test image.

True defect patches and pseudo defect patches are used for the learning with labelling.

Rectangle images cropped for the keypoint obtained using SURF are shown in Figure 5.

C. Feature Extraction Using CNN

Feature extraction is performed by inputting the image cropped using SURF in IV-B to CNN. AlexNet [6] is used as a pre-training model of CNN which structural concept is shown in Figure 6. Here, 4096-dimensional features which are obtained from the final layer of the fully connected layer

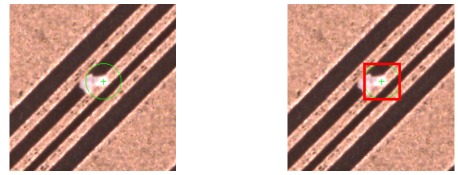

(a) Result of SURF (b) Cropped by rectangle

Figure 5. Cut by rectangle

(Layer FC7) are used for SVM learning as a transfer learning method.

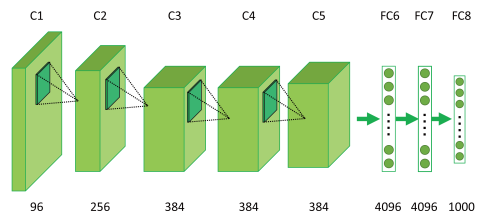

Figure 6. AlexNet

D. Construction of Classifier

SVM for defect detection is constructed using the defect patch and non-defect patch in the learning data. A linear kernel is used for defect detection SVM. The linear kernel is denoted by Equation (1).

$$k(\boldsymbol{x}_n, \boldsymbol{x}_m) = \boldsymbol{x}_n^T \boldsymbol{x}_m \tag{1}$$

The RBF kernel is used for constructing defect classification SVM. The RBF kernel is denoted by Equation (2). γ in Equation (2) is a parameter that controls the identification boundary. Here, as the value of γ increases, the boundary becomes more complicated.

$$k(\boldsymbol{x}_n, \boldsymbol{x}_m) = \exp(-\gamma \|\boldsymbol{x}_n - \boldsymbol{x}_m\|^2) \tag{2}$$

The performance of the final classification of the test image is shown in Table I according to the classification result using the classification SVM. It is important to reduce the rate of erroneously classifying a true defect as a pseudo defect.

TABLE I. FINAL JUDGMENT

Defect Patch in Image	Final Classification
Only True Defect Patch	True Defect
Only Pseudo Defect Patch	Pseudo Defect
True Defect Patch and Pseudo Defect Patch	Classify by Majority Voting
Non-Defect Patch	True Defect

V. EXPERIMENT

An experiment was performed to validate the effectiveness of the proposed method. Defect detection and defect classification are performed in two stages with the proposed method, that is, the experiment consists of detection and classification.

The dataset used for the experiment consists of 65 true defect images and 72 pseudo defect images.

 ISBN: 978-1-61208-534-0

A. Detection Experiment

The keypoints was detected by SURF on the defect image of the dataset, and SURF was obtained according to the number defined in the learning data in detection experiments. The results of obtained patches are shown in Table II.

TABLE II. NUMBER OF PATCH

Defect Patch	*Non-Defect Patch*
274	164

Detection and evaluation experiments were performed using the patch shown in Table II. The classifier is SVM, the kernel of SVM is a linear kernel, the parameter C of SVM is 1000 by GridSearch, and the evaluation method used is Leave-One-Out. Patches cropped from the same image were removed from the learning data for the test patch when Leave-One-Out is applied.

Precision, *Recall*, *F-measure* and *Accuracy* are calculated using the following equations.

$$
\begin{aligned}
Precision &= \frac{TP}{TP+FP} \\
Recall &= \frac{TP}{TP+FN} \\
F-measure &= \frac{2*Recall*Precision}{Recall+Precision} \\
Accuracy &= \frac{TP+TN}{TP+FP+FN+TN}
\end{aligned}
$$

TABLE III. EVALUATION OF DETECTION ACCURACY[%]

Precision	*Recall*	*F-measure*	*Accuracy*
89.05	84.14	86.52	82.64

It is confirmed that more than 80 percent of accuracy is obtained even without the reference image in inspection shown as Table 7.

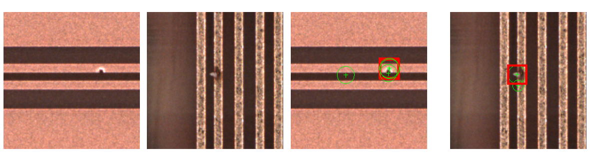

(a) True Defect (b) Pseudo Defect (c) Detect of True Defect (d) Detect of Pseudo Defect

Figure 7. Result of Detect

The detected images are shown in Figure 7. Figure 7(a) and Figure 7(b) show original images, and Figure 7(c) and Figure 7(d) show results of defect detection. The green circle in Figure 7 represents the keypoint that became a defect candidate. The red rectangle indicates the patch judged as a defect. It is shown from Figure 7 that the defect region can be cropped correctly.

B. Classification Experiment

The classification experiment was performed under the assumption that all detections made in V-A on the defect image of the dataset were successful. It is judged whether the patch is a true defect patch or a pseudo defect patch using only the defect patch from the cropped patch. The classifier is SVM, the kernel of SVM is RBF kernel, the parameter C of SVM is 1 by GridSearch, and the parameter γ of RBF kernel is 131. The evaluation method used is Leave-One-Out. The classification result of method [5] is shown when mask image is used at the test time for comparison. The number of learning images in the subset in method [5] is set to 50 as the number of datasets.

The result of classification are shown in Table IV.

TABLE IV. EVALUATION OF CLASSIFICATION ACCURACY[%]

Method	*Precision*	*Recall*	*F-measure*	*Accuracy*
Paper [5]	53.21	80.56	62.38	52.55
Proposed	86.11	67.39	75.61	70.80

It is confirmed that defect classification can be performed more accurately than method [5] despite using the defect detection method without reference images, which is shown from Table IV.

VI. CONCLUSION

This paper proposed a new highly accurate defect classification method without using reference images by introducing keypoint extraction and CNN feature extraction. The effectiveness of the proposed method was validated by an experiment for detecting the defect using actual images of electronic circuit boards. Defect detection without reference images was implemented by performing patch cropped using the keypoint extraction in the proposed method. As future work, there is higher accuracy of detection and classification.

ACKNOWLEDGMENT

Iwahori's research is supported by Japan Society for the Promotion of Science (JSPS) Grant-in-Aid for Scientific Research (C) (23500228) and Chubu University Grant.

REFERENCES

[1] S. Maeda, M. Ono, H. Kubota, and M. Nakatani, "Precise detection of short-circuit defects on tft substrate by infrared image matching," Systems and Computers in Japan, vol. 30, no. 12, 1999, pp. 72–84.

[2] M. Numada and H. Koshimizu, "A method for detecting globally distributed defects by using learning with mahalanobis distance," Journal of the Japan Society for Precision Engineering, vol. 75, no. 2, 2009, pp. 262–266.

[3] H. Rau and C.-H. Wu, "Automatic optical inspection for detecting defects on printed circuit board inner layers," The International Journal of Advanced Manufacturing Technology, vol. 25, no. 9-10, 2005, pp. 940–946.

[4] H. Inoue, Y. Iwahori, B. Kijsirikul, and M. Bhuyan, "Svm based defect classification of electronic board using bag of keypoints," in ITC-CSCC: International Technical Conference on Circuits Systems, Computers and Communications, 2015, pp. 31–34.

[5] H. Hagi, Y. Iwahori, S. Fukui, Y. Adachi, and M. K. Bhuyan, "Defect classification of electronic circuit board using svm based on random sampling," Procedia Computer Science, vol. 35, 2014, pp. 1210–1218.

[6] A. Krizhevsky, I. Sutskever, and G. E. Hinton, "Imagenet classification with deep convolutional neural networks," in Advances in neural information processing systems, 2012, pp. 1097–1105.